N⁶-methyladenosine RNA methylation regulators participate in malignant progression and have prognostic value in clear cell renal cell carcinoma

ZONGTAI ZHENG, SHIYU MAO, YADONG GUO, WENTAO ZHANG, JI LIU, CHENG LI and XUDONG YAO

Department of Urology, Shanghai Tenth People's Hospital, Tongji University School of Medicine, Shanghai 200072, P.R. China

Abstract. N⁶-methyladenosine (m6A) RNA methylation is the most prevalent type of mRNA modification; however, little is known about its function in clear cell renal cell carcinoma (ccRCC). The present study aimed to establish and validate a m6A-related risk signature as a prognostic factor for patients with ccRCC. Consensus clustering was used to divide patients with ccRCC from The Cancer Genome Atlas (TCGA) cohort (n=489) into three clusters (cluster 1/2/3) based on 19 m6A RNA methylation regulators. In addition, a m6A-related risk signature was constructed using TCGA data, and its accuracy was validated using data from the International Cancer Genome Consortium (n=91). The prognostic performance of the risk signature was evaluated by Kaplan-Meier analyses, least absolute shrinkage and selection operator Cox regression, multivariate Cox regression, receiver operating characteristic curves and nomograms. The results revealed that the majority of the 19 m6A RNA methylation regulators were differentially expressed among ccRCC stratified by different clinicopathological features. The cluster 1 group exhibited a higher frequency of metastasis and poorer overall survival compared with the cluster 2/cluster 3 group. The hallmarks of RNA metabolism, transcription misregulation in cancer and regulation of autophagy, were significantly enriched in the cluster 1 group. A m6A-related risk signature was constructed and validated with high prognostic accuracy for the prediction of 5-year survival and recurrence (area under the curve, 0.736 and 0.728, respectively). The present study also established robust nomograms for evaluating the risk of mortality and recurrence for patients with ccRCC (c-index, 0.783 and 0.819, respectively). The dysregulation of hub m6A RNA methylation regulator expression levels and m6A RNA methylation levels were also validated in multiple RCC cells using *in vitro* experiments. Taken together, the m6A RNA methylation regulators promoted the malignant progression of ccRCC and exhibited good performance in prognostic predictions. These results provided insight into the development of m6A-targeted treatments for ccRCC.

Introduction

Currently, there are 163 reported post-transcriptional modifications of RNAs, including mRNA, tRNA, rRNA, snRNA and others (1). These processes can directly influence the structure of RNAs, which ensures a diversity of functions. The modifications of mRNAs, such as N¹-methyladenosine, N⁶-methyladenosine (m6A), N⁷-methylguanosine, 5-methylcytosine and 2'-O-methylation, serve fundamental roles in the regulation of gene expression (2-4). Among these, the m6A RNA modification is the most prevalent post-transcriptional modification of internal mRNA in eukaryotes, accounting for 0.1-0.4% of total adenosine residues (5).

Although m6A modification has been known for over four decades (6), its distribution and function were largely unexplored until the development of m6A RNA immunoprecipitation sequencing (7,8). Preferentially enriched around stop codons and the long internal exons in the 3'-untranslated region, m6A RNA methylation is evolutionarily conserved between human and mouse, indicating an essential role for this modification (7,8).

The status of m6A RNA methylation is mainly regulated by m6A RNA methylation regulators; ≥20 m6A RNA methylation regulators have been identified and termed 'writers', 'erasers' and 'readers' (5,9-11). 'Writers' refer to m6A methyltransferases including Wilms tumor 1-associated protein (WTAP),

zinc finger CCCH domain-containing protein 13 (ZC3H13), KIAA1429, methyltransferase like 3 (METTL3), METTL14 and RNA-binding motif protein 15 (RBM15). 'Erasers' are demethylases including Fat mass and obesity-associated protein (FTO), alkB homolog 3 (ALKBH3) and ALKBH5. 'Readers' function as binding proteins and include YTH domain-containing 1 (YTHDC1), YTHDC2, YTH N^6-methyladenosine RNA binding protein 1 (YTHDF1), YTHDF2, YTHDF3, insulin-like growth factor 2 mRNA-binding protein 1 (IGF2BP1), IGF2BP2, IGF2BP3, heterogeneous nuclear ribonucleoprotein C (HNRNPC), heterogeneous nuclear ribonucleoprotein A2/B1 (HNRNPA2B1) and RNA binding motif protein X-linked (RBMX). The interactions among m6A RNA methylation regulators contribute to the dynamic role of m6A methylation in multiple physiological processes, including stem cell renewal, differentiation, carcinogenesis, neurogenesis, circadian clock functions and DNA damage response (12-15).

Increasing evidence has suggested that dysregulated expression of m6A RNA methylation regulators affects the initiation and progression of cancers, such as glioblastoma (16,17), acute myeloid leukemia (AML) (18), hepatocellular carcinoma (19) and breast cancer (20). Recently, m6A RNA methylation regulator expression levels were demonstrated to be effective biomarkers for discrimination among RCC subtypes (21), and genetic alterations of m6A RNA methylation regulators contributed to malignant progression and poor clinical characteristics in patients with clear cell renal cell carcinoma (ccRCC) (22). In addition, studies revealed that the levels of m6A RNA methylation were decreased in ccRCC tissues compared with adjacent non-tumor tissues, which promoted the invasion and migration of renal cancer cells and led to poor prognoses in patients with ccRCC (10,22,23). Despite recent advances, a limited number of studies have comprehensively explored the expression of m6A methylation regulators in patients with ccRCC (21,24) exhibiting different clinicopathological features, their involvement in malignant progression and prognostic predictions. In addition, which m6A RNA methylation regulators may be more suitable for prognostic stratification in ccRCC has not been investigated.

The present study aimed to examine the expression of 19 RNA methylation regulators in a comprehensive manner with the clinicopathological features and RNA sequencing data of a ccRCC cohort from The Cancer Genome Atlas (TCGA) to explore the association between the gene expression and clinicopathological features. In addition, the present study aimed to construct a m6A-related risk signature and nomograms for prognostic prediction. Finally, this study aimed to detect the expression of seven hub m6A RNA methylation regulators and m6A RNA modification levels in RCC cell lines and a normal renal tubular epithelial cell line.

Materials and methods

Data processing. The mRNA (RNA sequencing) Fragments Per Kilobase of transcript per Million Fragments standardized expression data and corresponding clinicopathological features were retrieved for 489 ccRCC tissues and 72 adjacent non-tumor tissues from TCGA (http://cancergenome.nih.gov/) and 91 ccRCC tissues from the International Cancer Genome Consortium (ICGC; https://icgc.org/). Patients without prognostic information were excluded from analysis. Overall survival (OS)

and disease-free survival (DFS) were the primary end points of this study. OS was defined as the time between diagnosis and death or was censored at the last follow-up. DFS was defined as the time between diagnosis or surgery and the recurrence of disease or death (for any reason) at the last follow-up.

m6A RNA methylation regulators. A total of 19 m6A RNA methylation regulators that were available in TCGA and ICGC cohorts were selected. The expression of 19 m6A RNA methylation regulators was systematically compared in 539 ccRCC tissues with different pathological features and with 72 adjacent non-tumor tissues.

Bioinformatics analyses. To identify the optimal molecular subgroups, the present study divided patients with ccRCC into different clusters by applying the 'ConsensusClusterPlus' package in R v.1.50.0 (http://www.bioconductor.org/packages/release/bioc/html/ConsensusClusterPlus.html) based on the expression of the 19 m6A RNA methylation regulators. The resampling program was used to sample 80% of the samples 50 times; the similarity distance between samples was estimated by the Euclidean distance (25), and 'km dist' was used as the clustering algorithm to select the reliable and stable subgroup classification. The criteria to determine the optimal number of clusters were a relatively high consistency between clusters and no appreciable rise in the area under the cumulative distribution function curve. The 'proportion of ambiguous clustering' was used to select an optimal value of clusters (k value) (26). Venn online software (http://bioinformatics.psb.ugent.be/webtools/Venn/) was used to identify the overlapping differentially expressed genes (DEGs) between clusters. Kyoto Encyclopedia of Genes and Genomes (KEGG) pathway enrichment and Gene Ontology (GO) analyses were performed and visualized using the Database for Annotation, Visualization and Integrated Discovery software (DAVID; version 6.7; http://david.abcc.ncifcrf.gov/home.jsp) to provide comprehensive pathway interpretations and functional annotation of DEGs (|log$_2$FC|>2 and adjusted P value <0.05) between different clusters. Search Tool for the Retrieval of Interacting Genes software (STRING; https://string-db.org/) was used to analyze the interactions and evaluate the level of interactions (including interactions determined by experiments or obtained from curated databases, and interactions determined by text mining or co-expression analyses) among the m6A RNA methylation regulators.

Univariate Cox regression analysis was used to identify the prognostic value of the expression of the m6A RNA methylation regulators in the training cohort (TCGA). Regulators associated with OS in univariate analyses were subsequently selected for least absolute shrinkage and selection operator (LASSO) Cox regression to construct a m6A-related risk signature for clinical prognosis (27). As a result, seven m6A RNA methylation regulators with their corresponding coefficients were determined by the minimum mean cross-validated error, choosing the optimal penalty parameter λ related to the minimum 10-fold cross validation within the training set. The risk score of each patient with ccRCC in the training and validation (ICGC) cohorts was calculated using the following formula:

$$Risk\ score = \sum_{i=1}^{n} Coef_i \times x_i$$

Where x_i is the standardized expression value of each selected m6A RNA methylation regulator, and $Coef_i$ is the corresponding coefficient of the gene. All patients were divided into low- and high-risk groups based on the median value of the risk scores in the training and validation cohorts.

Cell culture. The human RCC cell lines SW839, SN12C, 786-O and OSRC-2 and human normal renal tubular epithelial cell line HK-2 were obtained from Cell Bank of the Chinese Academy of Sciences. The human RCC cell lines were cultured in RPMI-1640 (Gibco; Thermo Fisher Scientific, Inc.) with 10% FBS (HyClone; GE Healthcare Life Sciences) and 1% penicillin/streptomycin (P/S; Gibco; Thermo Fisher Scientific, Inc.). HK-2 cells were cultured in Keratinocyte Medium (ScienCell Research Laboratories, Inc.) with 1% Keratinocyte Growth Supplement (ScienCell Research Laboratories, Inc.) and 1% P/S (ScienCell Research Laboratories, Inc.). All cells were cultured at 37°C in 5% CO_2.

RNA isolation and reverse transcription-quantitative PCR (RT-qPCR). Total RNA was isolated from cells using TRIzol® reagent (Invitrogen; Thermo Fisher Scientific, Inc.) according to the manufacturer's instructions. Reverse transcription was performed using SuperScript III Reverse Transcriptase (Invitrogen; Thermo Fisher Scientific, Inc.) according to the manufacturer's instructions, and qPCR was performed using a SYBR® Green PCR Master Mix (Applied Biosystems; Thermo Fisher Scientific, Inc.) and a 7900HT Fast Real-Time PCR System (Applied Biosystems; Thermo Fisher Scientific, Inc.). The thermocycling conditions were as follows: 95°C for 10 min, followed by 40 cycles of 95°C for 10 sec and at 60°C for 1 min. Relative mRNA levels were normalized against β-actin. Data were analyzed using the $2^{-\Delta\Delta Cq}$ method (28). Primer sequences are presented in Table SI.

Total m6A RNA modification detection. Total m6A RNA modification was detected in 200 ng aliquots of total RNA extracted from cells using the EpiQuik m6A RNA Methylation Quantification Kit (EpiGentek Group, Inc.) according to the manufacturer's instructions. Briefly, total RNA was bound to wells using the RNA Binding Solution. m6A RNA modification was detected using capture and detection antibodies. The detected signal was enhanced and quantified by reading absorbance at 450 nm using a microplate reader (BioTek Instruments, Inc.). The amount of m6A RNA modification was proportional to the OD intensity. The experiments were performed in triplicate.

Statistical analysis. The differences in the expression levels of m6A RNA methylation regulators between ccRCC tissues and adjacent non-tumor tissues were compared using Wilcoxon test. Differences in the expression levels of m6A RNA methylation regulators and m6A RNA modification levels between HK-2 and human RCC cell lines were analyzed using one-way ANOVA followed by Dunnett's post-hoc test. The distributions of age, sex, histological grade and TNM stage between clusters and between risk subgroups were analyzed using the Kruskal-Wallis test and the Chi-square test, respectively. One-way ANOVA was performed to compare the risk scores in ccRCC with different T stages. Student's t-test was employed to compare the risk scores in patients grouped by

Table I. Clinicopathological characteristics of patients in TCGA and ICGC cohorts.

	TCGA cohort		ICGC cohort	
Characteristic	Number	%	Number	%
Age, years				
>65	169	34.6	28	30.8
≤65	320	65.4	63	69.2
Sex				
Male	323	66.1	52	57.1
Female	166	33.9	39	42.9
Pathological stage				
I	238	48.7	52	57.1
II	51	10.4	13	14.3
III	120	24.5	15	16.5
IV	80	16.4	9	9.9
NA	0	0	2	2.2
Histological grade				
G1	10	2.0	NA	NA
G2	211	43.1		
G3	195	39.9		
G4	73	14.9		
T stage				
T1	244	49.9	54	59.3
T2	62	12.7	13	14.3
T3	172	35.2	22	24.2
T4	11	2.2	2	2.2
N stage				
N0	232	47.4	85	93.4
N1	14	2.9	2	2.2
Nx	243	49.7	4	4.4
M stage				
M0	412	84.3	81	89
M1	77	15.7	9	9.9
Mx	0	0	1	1.1

TCGA, The Cancer Genome Atlas; ICGC, International Cancer Genome Consortium; NA, not available.

binary clinical variables. Univariate and multivariate Cox regression analyses were performed to identify the prognostic value of the risk score and other clinicopathological features. Comparisons of survival between the clusters or risk groups were performed using Kaplan-Meier curves with the log-rank test, followed by pairwise comparisons between clusters using the 'survminer' R package v.0.4.6 with Bonferroni correction. Receiver operating characteristic curves (ROCs) were used to test the prediction accuracy of the risk score and clinicopathological features for 5-year survival and recurrence. Variables significant in the multivariate Cox regression analyses were used to construct prognostic nomograms validated by the concordance index (c-index) and calibration plots using the 'Rms' package (https://cran.r-project.org/web/packages/rms/index.html) in R. SPSS 22.0 (IBM Corp.), GraphPad Prism 6
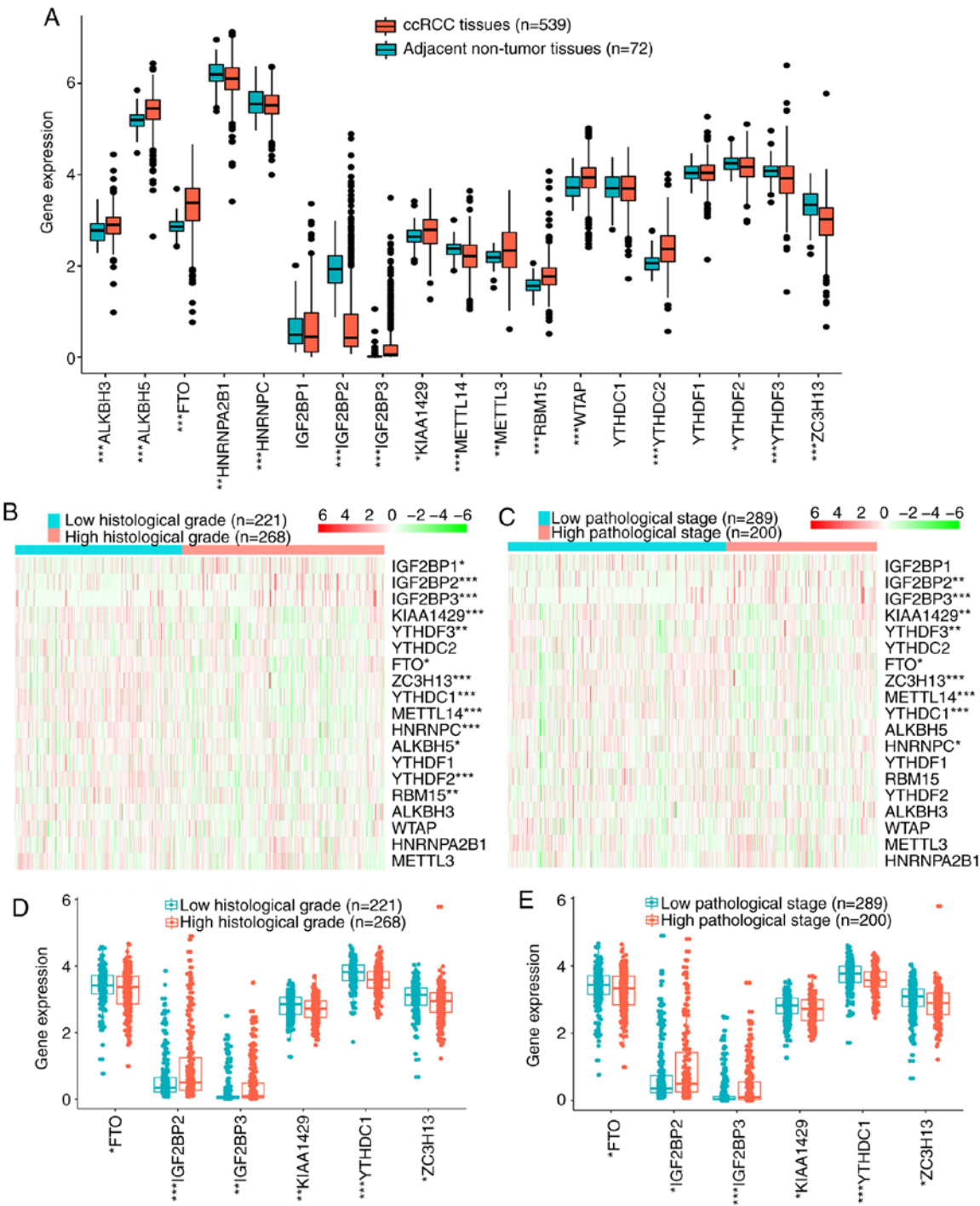
Figure 1. Expression of m6A RNA methylation regulators. (A) Expression levels of 19 m6A RNA methylation regulators in ccRCC and adjacent non-tumor tissues. (B and C) Heat maps of expression levels of 19 m6A RNA methylation regulators in ccRCC with different (B) histological grades or (C) pathological stages. (D and E) Expression levels of FTO, IGF2BP2, IGF2BP3, KIAA1429, YTHDC1 and ZC3H13 in ccRCC with different (D) histological grades or (E) pathological stages. *P<0.05, **P<0.01, ***P<0.001. m6A, N[6]-methyladenosine; ccRCC, clear cell renal cell carcinoma; FTO, fat mass and obesity-associated protein; YTHDC1, YTH domain-containing 1; IGF2BP, insulin-like growth factor 2 mRNA-binding protein; ZC3H13, zinc finger CCCH-type-containing 13.

(GraphPad Software, Inc.) and R v3.6.1 (https://www.r-project. org/) were used for statistical analysis. P<0.05 was considered to indicate a statistically significant difference, with a Bonferroni correction (p<0.05/3) applied for pairwise comparisons.

Results

Associations among the expression of m6A RNA methylation regulators and clinicopathological features. Among 19 m6A

RNA methylation regulators, 15 DEGs were identified, including 9 upregulated and 6 downregulated genes in 539 ccRCC tissues compared with 72 adjacent non-tumor tissues in TCGA cohort (Fig. 1A), which indicated that m6A RNA methylation regulators exerted important biological functions in the tumorigenesis of ccRCC. The main clinicopathological characteristics of patients with ccRCC are presented in Table I. In the present study, G1-G2 was defined as low histological grade, G3-G4 was defined as high histological grade, stage I-II was defined as low
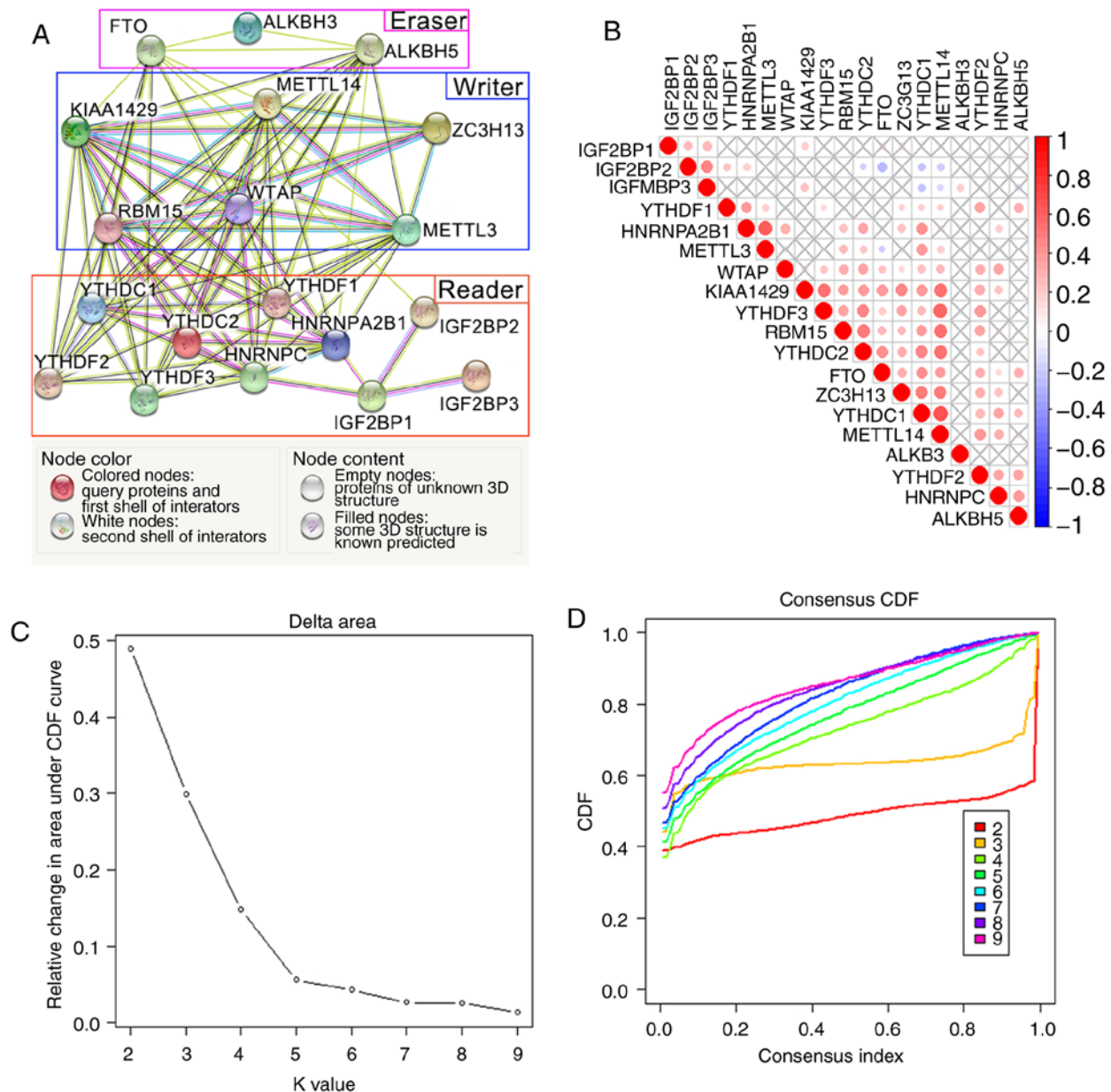
Figure 2. Interaction among m6A RNA methylation regulators and differential clinicopathological features of patients with clear cell renal cell carcinoma in cluster 1/2/3 subgroups. (A) Network and (B) correlations among 19 m6A RNA methylation regulators. (C) Consensus clustering CDF and (D) relative change in area under CDF curve for k=2-10.

pathological stage, and stage III-IV was defined as high pathological stage. The associations between the expression levels of m6A regulatory regulators and the clinicopathological features of ccRCC, including histological grade and pathological stage, were analyzed in TCGA cohort. The results demonstrated that the expression of most m6A RNA methylation regulators was significantly associated with histological grade (Fig. 1B) and pathological stage (Fig. 1C). In addition, different expression levels of FTO, IGF2BP2, IGF2BP3, KIAA1429, YTHDC1 and ZC3H13 were identified by quantitative analyses according to histological grade or pathological stage (Fig. 1D and E). These results suggested that the m6A RNA methylation regulators contributed to the malignant progression of ccRCC.

Associations among the m6A RNA methylation regulators. The network and correlation analyses among 19 m6A RNA

methylation regulators were conducted to determine their interactions (Fig. 2A and B). 'Writers' had a wide range of interactions, including interactions determined by experiments or obtained from curated databases, with the m6A RNA methylation regulators. In addition, the 'writers' METTL14, KIAA1429, WTAP, RBM15 and ZC3H13 were co-expressed with more than half of the 19 m6A RNA methylation regulators. Based on these results, 'writers' were considered to be the hub gene set in the network.

WTAP was the only 'writer' with various known interactions with the other five 'writers', revealing that it may be a hub gene of the 'writers'. WTAP expression was also positively associated with the 'writers' KIAA1429, ZC3H13 and RBM15 in ccRCC (Fig. 2B). In addition, the expressions levels of KIAA1429, YTHDF3, RBM15, YTHDC2, FTO, ZC3H13, YTHDC1, METTL14 and YTHDF2 were positively associated with each other.
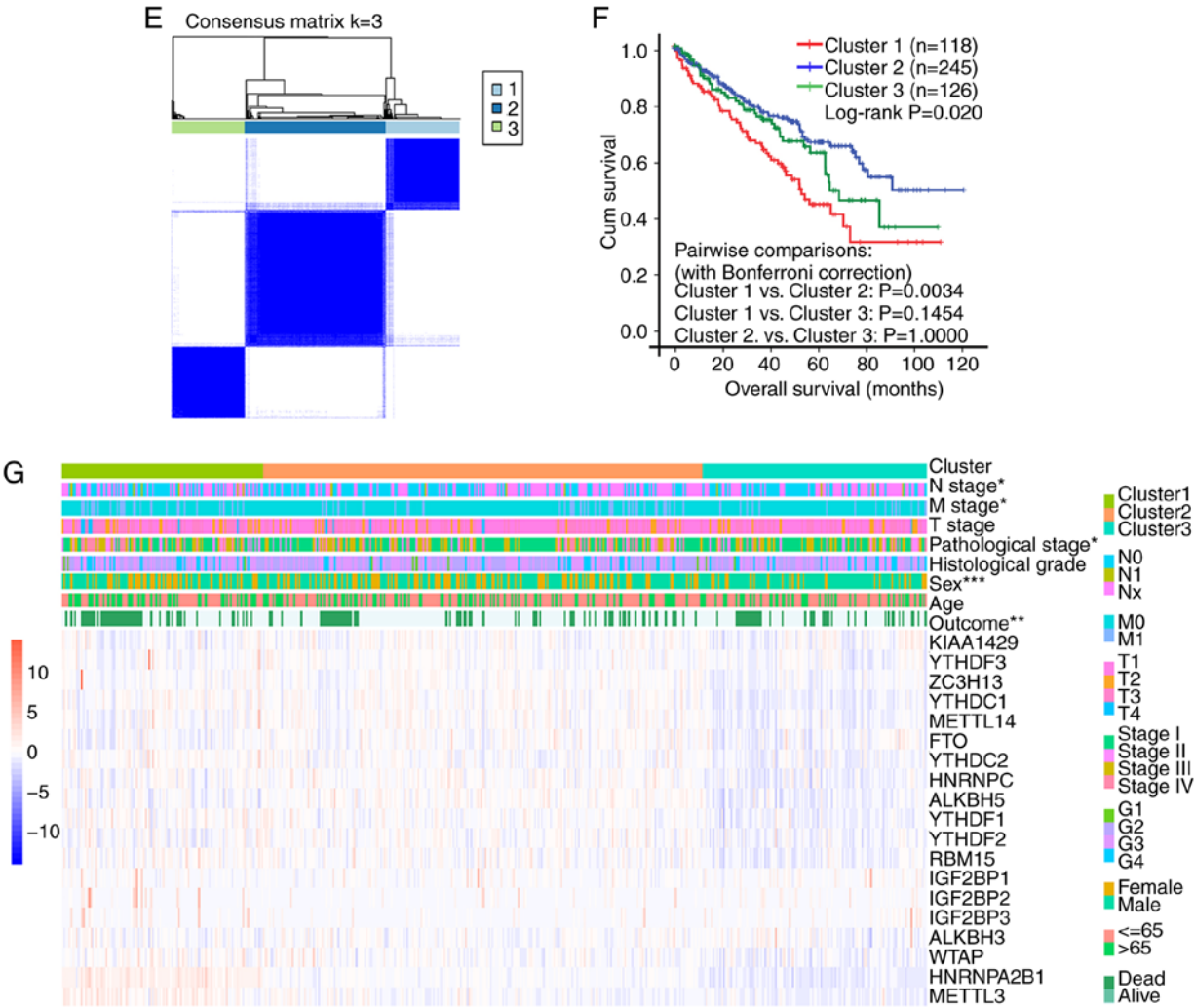
Figure 2. Continued. Interaction among m6A RNA methylation regulators and differential clinicopathological features of patients with clear cell renal cell carcinoma in cluster 1/2/3 subgroups. (E) Consensus clustering matrix for k=3. (F) Kaplan-Meier overall survival curves of the three clusters. (G) Clinicopathological features of the three clusters. *P<0.05, **P<0.01, ***P<0.001. m6A, N^6-methyladenosine; CDF, cumulative distribution function.

By contrast, the interactions between 'erasers' and other regulators were identified by text mining or co-expression analyses, but lacked known interactions. With the exception of FTO, the 'erasers' ALKBH3 and ALHBH5 lacked co-expression with other m6A RNA methylation regulators. Independent interaction groups were identified within the 'readers', indicating the diverse functions of the 'readers'; YTHDC1, YTHDC2, YTHDF1, IGF2BP2 and HNRNPA2B1 exhibited co-expression with each other in ccRCC.

Clinicopathological features and biological processes of three clusters of patients with ccRCC. According to the 'proportion of ambiguous clustering' method and the criteria for selecting the number of clusters, k=3 was selected as the optimal value in TCGA cohorts (Fig. 2C-E). Thus, the patients from TCGA cohort were divided into three clusters, namely cluster 1, 2 and 3. Differences in clinicopathological features and survival distributions between different clusters were identified, with the expression values of the m6A RNA methylation regulators screened out as heatmaps (Fig. 2F). Cluster 1/2/3 subgroups were significantly associated with sex (P<0.001), M stage (P=0.048), N stage (P=0.039), pathological stage (P=0.021) and survival outcome (P<0.001)

(Table II). Additionally, patients in cluster 1 exhibited the shortest OS (P=0.02), followed by cluster 3 and cluster 2 (Fig. 2G). These results revealed that patients with ccRCC in different clusters exhibited significantly diverse clinicopathological features, and the clustering results were associated with survival.

To identify different biological processes among the three clusters, DEGs were identified among the clusters, and their pathway interpretations and functional annotations were visualized. As pathological features between cluster 2 and cluster 3 were similar, and patients with ccRCC in cluster 1 exhibited the worst survival outcomes among all clusters and largely different clinicopathological features from cluster 2 and cluster 3, DEGs between cluster 1 and cluster 2 and between cluster 1 and cluster 3 were investigated. A total of 1,386 DEGs (736 upregulated and 650 downregulated) were identified between cluster 1 and cluster 2, and 2,287 DEGs (1,756 upregulated and 531 downregulated) were identified between cluster 1 and cluster 3. Venn online software was used to identify the overlapping DEGs between the two groups of DEGs (Fig. 3A and B). As a result, 603 upregulated and 149 downregulated overlapping DEGs were selected and analyzed by DAVID software to perform GO enrichment and KEGG pathway analyses.

Table II. Clinicopathological features between clusters in The Cancer Genome Atlas cohort.

Characteristic	Cluster 1, n (%)	Cluster 2, n (%)	Cluster 3, n (%)	P-value
Age, years				
>65	46 (39.0)	80 (32.7)	43 (34.1)	0.453
≤65	72 (61.0)	165 (67.3)	83 (65.9)	
Sex				
Male	70 (59.3)	151 (61.6)	102 (19.0)	<0.001[c]
Female	48 (40.7)	94 (38.4)	24 (81.0)	
Pathological stage				
I	47 (39.8)	127 (51.8)	64 (50.8)	0.021[a]
II	17 (14.4)	20 (8.2)	14 (11.1)	
III	27 (22.9)	60 (24.5)	33 (26.2)	
IV	27 (22.9)	38 (15.5)	15 (11.9)	
Histological grade				
G1	3 (2.5)	6 (2.4)	1 (0.8)	0.058
G2	44 (37.3)	117 (47.8)	50 (39.7)	
G3	49 (41.5)	92 (37.6)	54 (42.9)	
G4	22 (18.6)	30 (12.2)	21 (16.7)	
T stage				
T1	49 (41.5)	129 (52.7)	66 (52.4)	0.058
T2	20 (16.9)	25 (10.2)	17 (13.5)	
T3	43 (36.4)	87 (35.5)	42 (33.3)	
T4	6 (5.1)	4 (1.6)	1 (0.8)	
N stage				
N0	56 (47.5)	120 (49.0)	56 (44.4)	0.039[a]
N1	6 (5.1)	4 (1.6)	4 (3.2)	
Nx	56 (47.5)	121 (49.4)	66 (52.4)	
M stage				
M0	92 (78.0)	209 (85.3)	111 (88.1)	0.048[a]
M1	26 (22.0)	36 (14.7)	15 (11.9)	
Outcome				
Alive	64 (54.2)	179 (73.1)	85 (67.5)	0.002[b]
Dead	54 (45.8)	66 (26.9)	41 (32.5)	

[a]$P<0.05$, [b]$P<0.01$, [c]$P<0.001$, Kruskal-Wallis test.

The results of GO biological processes analysis demonstrated that upregulated and downregulated overlapping DEGs were mainly enriched in RNA metabolism, including 'RNA export from the nucleus', 'mRNA export from the nucleus', 'RNA processing', 'regulation of RNA splicing', 'mRNA splice site selection' and 'translation' (Fig. 3C and E). In KEGG pathway analysis, similar changes were observed in the corresponding signaling pathways, including 'spliceosome', 'ribosome', 'transcriptional misregulation in cancer', 'mRNA surveillance pathway' and other malignancy-related pathways including 'primary immunodeficiency', 'regulation of autophagy' and 'response to oxidative stress' (Fig. 3D and F). These results suggested that cluster 1/2/3 subgroups were associated not only with the clinicopathological features and survival, but also with malignancy-related biological processes.

Survival analysis of the m6A RNA methylation regulators in patients with ccRCC. The prognostic significance of the m6A

RNA methylation regulators in patients with ccRCC was further analyzed. In TCGA cohort, univariate Cox regression analysis identified 14 and 11 m6A RNA methylation regulators significantly associated with OS and DFS, respectively (Fig. 4A and B). Among the 14 m6A RNA methylation regulators in OS, six regulators were associated with poor OS (IGF2BP1, IGF2BP2, IGF2BP3, HNRNPA2B1, METTL3 and ALKBH3), and eight were associated with favorable OS (YTHDF2, YTHDF3, FTO, YTHDC1, YTHDC2, ZC3H13, KIAA1429 and METTL14). For DFS, two regulators were associated with poor DFS (IGF2BP2 and IGF2BP3), and nine regulators were associated with favorable DFS (YTHDF1, YTHDF2, YTHDF3, YTHDC1, YTHDC2, ZC3H13, KIAA1429, METTL14 and RBM15). The prognostic values of the m6A RNA methylation regulators in patients with different histological grades and pathological stages in TCGA cohort were subsequently analyzed by univariate Cox regression. In both low and high histological grade ccRCC, IGF2BP3 (P=0.030 and P<0.001, respectively) and
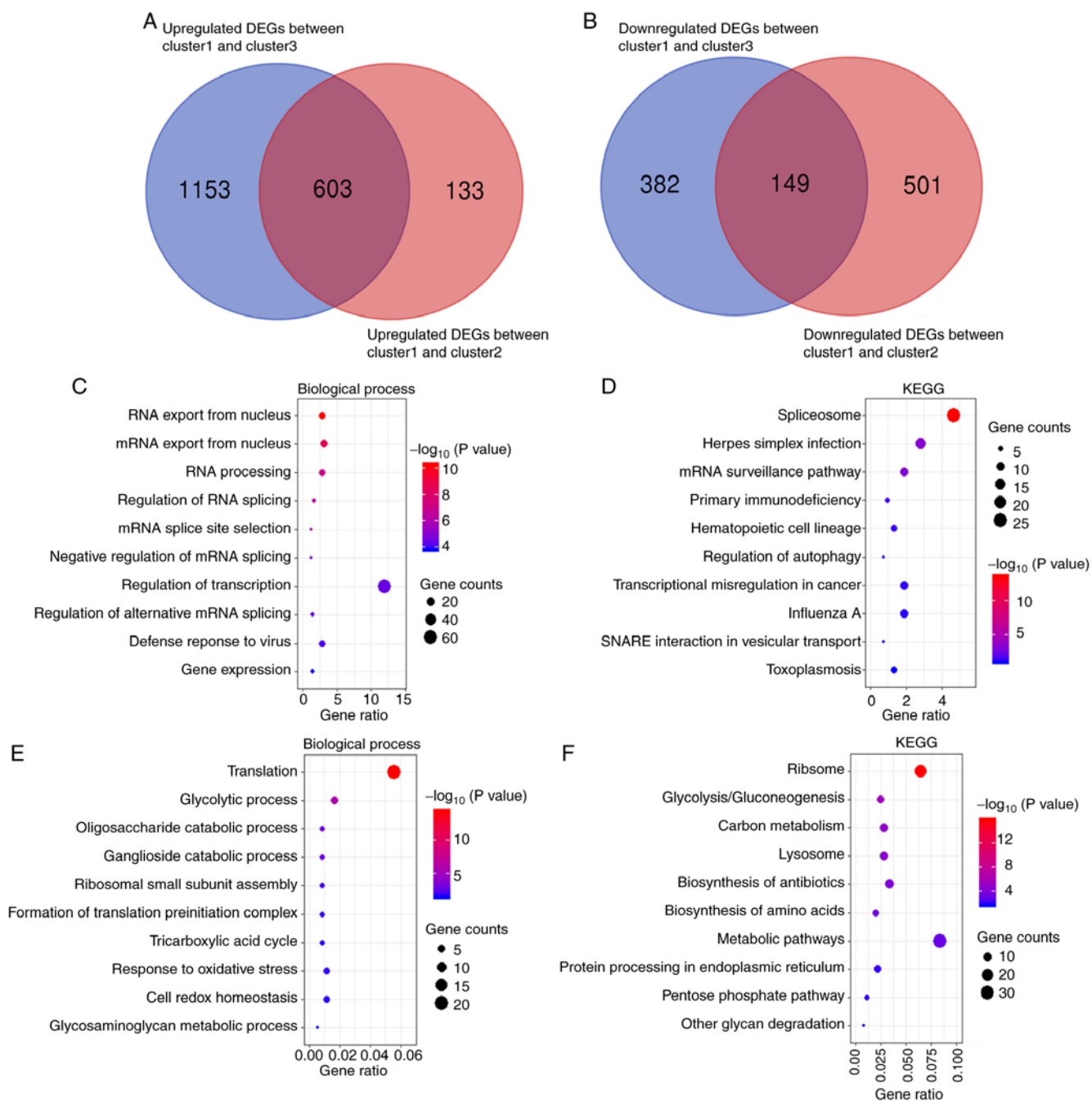
Figure 3. Functional annotation of ccRCC in three clusters. Venn software identified (A) 603 upregulated overlapping DEGs and (B) 149 downregulated overlapping DEGs between clusters 1/3 and 1/2. Functional annotation of upregulated overlapping DEGs using (C) Gene Ontology biological processes and (D) KEGG pathway analysis. Functional annotation of downregulated overlapping DEGs using (E) Gene Ontology biological processes and (F) KEGG pathway analysis. ccRCC, clear cell renal cell carcinoma; DEGs, differential expressed genes; KEGG, Kyoto Encyclopedia of Genes and Genomes.

KIAA1429 (P=0.045 and P=0.031, respectively) were significantly associated with OS; in both low and high pathological stage, METTL14 was significantly associated with OS (P=0.035 and P=0.003, respectively) (Fig. S1).

Construction and validation of the m6A-related risk signature based on the m6A RNA methylation regulators. Since the OS data was available in both TCGA and ICGC cohorts, the OS-associated m6A RNA methylation regulators in TCGA cohort were used to construct a m6A-related risk signature, and its accuracy was validated in the ICGC cohort. As a result, seven genes (IGF2BP2, IGF2BP3, METTL3, METTL14, HNRNPA2B1, KIAA1429

and ALKBH3) were identified by LASSO Cox regression in the training cohort (TCGA) to build the m6A-related risk signature (Fig. 4C and D). Subsequently, the risk score of each patient with ccRCC in the two cohorts was calculated using these seven genes and the formula presented in Materials and methods. Patients with ccRCC from the two cohorts were divided into low- and high-risk subgroups based on the median risk score. In TCGA cohort, the Kaplan-Meier method revealed that patients with high risk scores exhibited shorter OS (P<0.001; Fig. 4F) and DFS (P<0.001, Fig. 4G) compared with those with low risk scores. In the ICGC cohort, patients with high risk scores also exhibited shorter OS (P=0.005; Fig. 4H) compared with those with low risk scores.
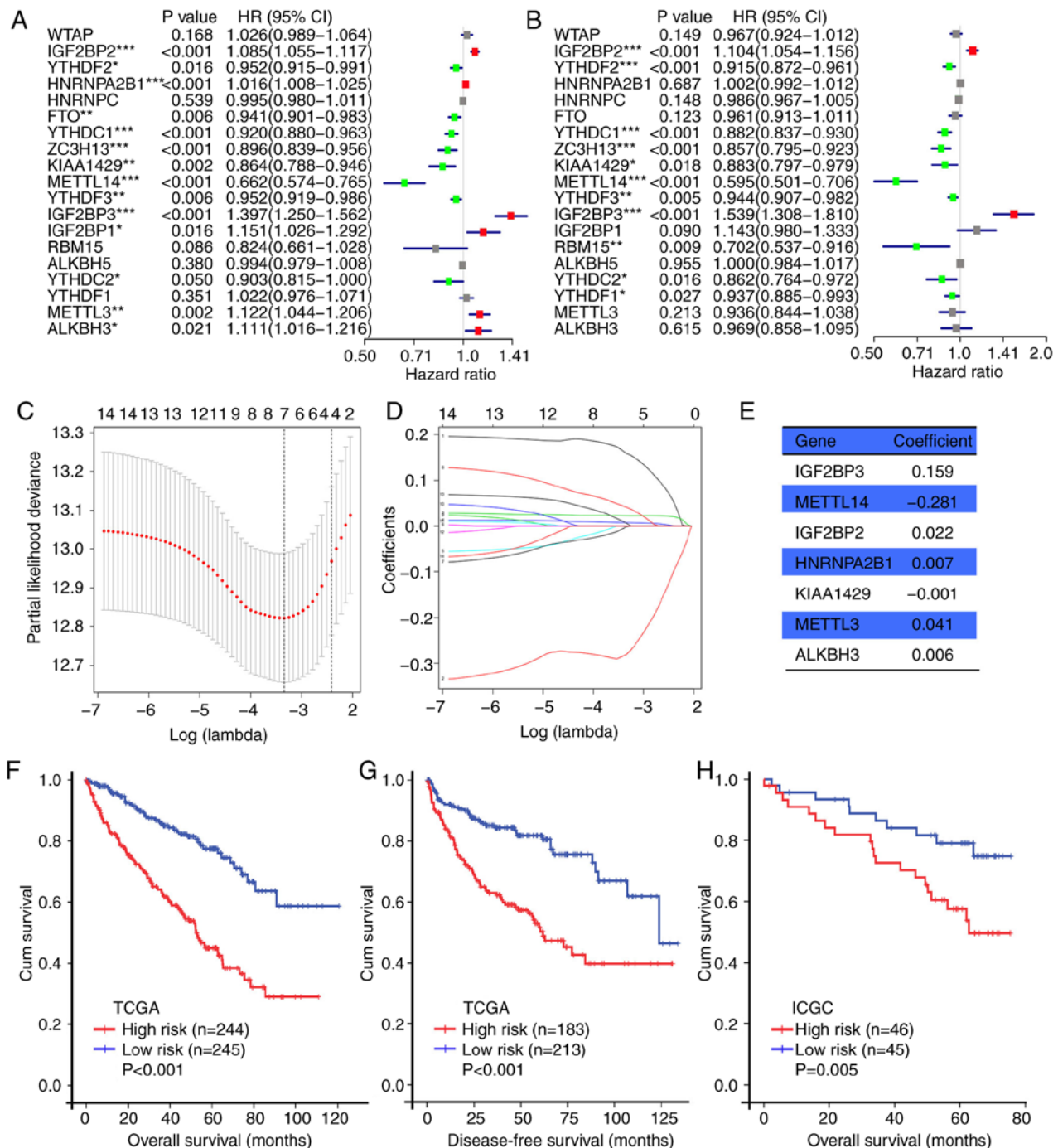
Figure 4. Prognostic value of m6A RNA methylation regulators in ccRCC. (A) OS-associated m6A RNA methylation regulators in TCGA cohort. (B) DFS-associated m6A RNA methylation regulators in TCGA cohort. (C) Plots of the cross-validation error rates in TCGA cohort. (D) Distribution of LASSO coefficients of 14 m6A RNA methylation regulators. (E) Coefficient values of each of the seven selected genes. (F and G) Kaplan-Meier OS and DFS curves for patients in TCGA cohort assigned to the high- and low-risk groups. (H) Kaplan-Meier OS curve for patients in the ICGC cohort assigned to the high- and low-risk groups. *P<0.05, **P<0.01, ***P<0.001. m6A, N6-methyladenosine; ccRCC, clear cell renal cell carcinoma; OS, overall survival; DFS, disease-free survival; TCGA, The Cancer Genome Atlas; ICGC, International Cancer Genome Consortium; HR, hazard ratio; CI, confidence interval; LASSO, least absolute shrinkage and selection operator.

Survival analyses were performed to compare the two risk groups of patients with different histological grades and pathological stages. In TCGA cohort, patients in the high-risk group exhibited poor OS and DFS compared with patients in the low-risk group regardless of histological grade and pathological stage (Fig. S2A-H). In the ICGC cohort, patients with high risk scores exhibited shorter OS compared with patients with low risk scores with a low pathological stage, but not a high pathological

stage (P=0.001 and P=0.549, respectively; Fig. S2I and J). ICGC data of histological grade and DFS were unavailable.

Based on these results, the risk signature derived from the seven m6A regulators was identified to be a powerful prognostic tool for patients with ccRCC. Further research is needed to evaluated whether the prognostic value of the risk signature was also independent of the known prognostic factors, such as histological grade and pathological stage.
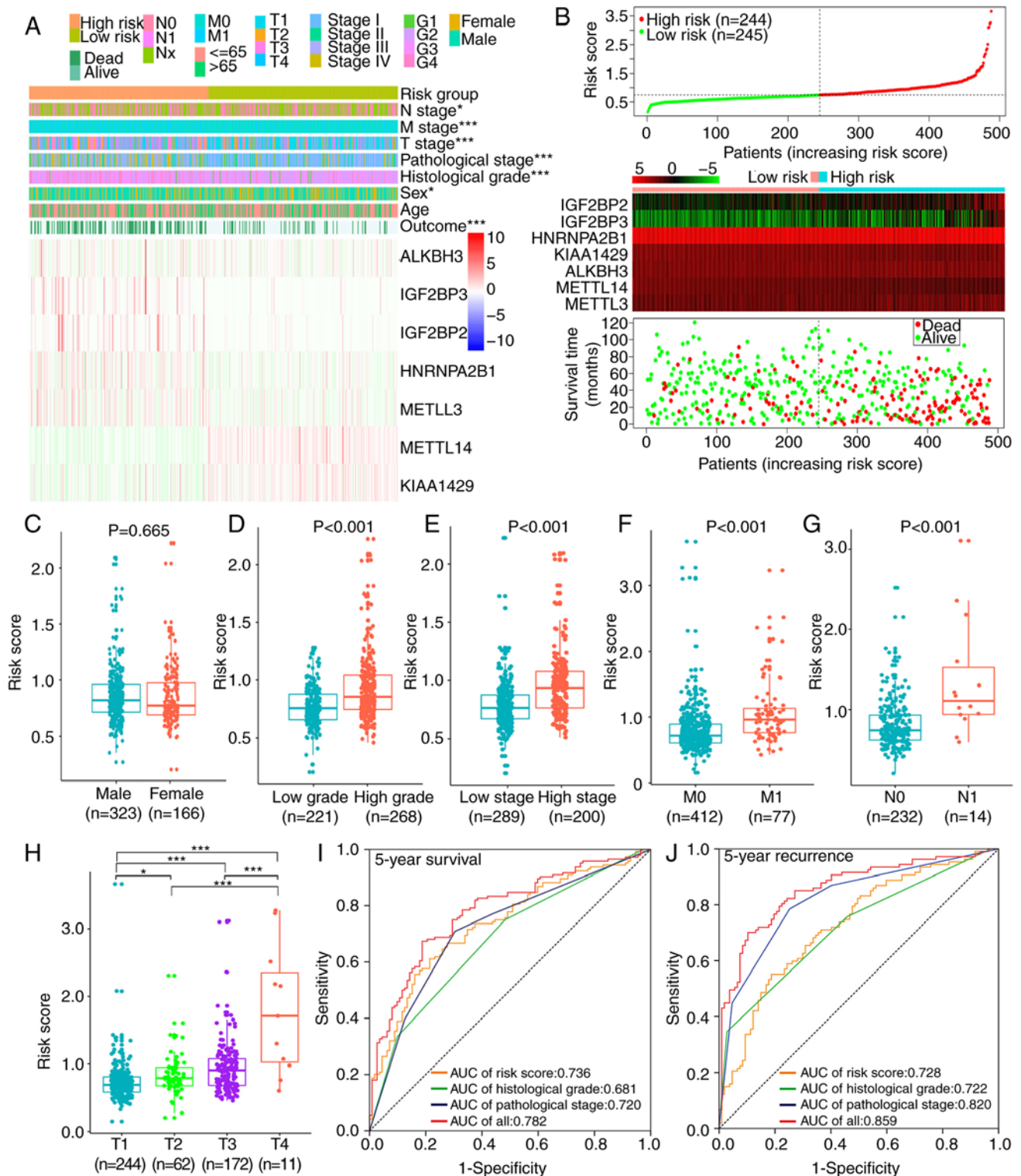
Figure 5. Associations among risk scores, clinicopathological features and prognoses in TCGA cohort. (A) Clinicopathological features and expression levels of seven m6A RNA methylation regulators were compared between the low- and high-risk groups. (B) Risk score, expression heat maps of seven m6A RNA methylation regulators and distribution of patient survival status between the low- and high-risk groups. (C-H) Distribution of risk scores stratified by (C) sex, (D) histological grade, (E) pathological stage, (F) M stage, (G) N stage and (H) T stage. (I and J) ROCs for risk scores, histological grade, pathological stage and their combination for (I) 5-year survival and (J) 5-year recurrence. *P<0.05, ***P<0.001. TCGA, The Cancer Genome Atlas; m6A, N6-methyladenosine; ROC, receiver operating characteristic; AUC, area under the curve.

Associations between the prognostic risk scores and clinico-pathological features. The heat map of the expression levels of the seven selected m6A RNA methylation regulators in the high- and low-risk subgroup patients in TCGA cohort is presented in Fig. 5A and B. Patients in the high-risk group had a higher proportion of males (P=0.015), higher pathological stage (P<0.001), higher histological grade (P<0.001), higher T stage (P<0.001), higher M stage (P<0.001), higher N

Table III. Clinicopathological characteristics in the low- and high-risk groups in The Cancer Genome Atlas cohort.

Characteristic	Low-risk group, n (%)	High-risk group, n (%)	P-value
Age, years			
>65	86 (35.1)	83 (34.0)	0.801
≤65	159 (64.9)	161 (66.0)	
Sex			
Male	151 (61.6)	172 (70.5)	0.039[a]
Female	94 (38.4)	72 (70.5)	
Pathological stage			
I	154 (62.9)	84 (34.4)	<0.001[b]
II	25 (10.2)	26 (10.7)	
III	47 (19.2)	73 (29.9)	
IV	19 (7.8)	61 (25.0)	
Historical grade			
G1	8 (3.3)	2 (0.8)	<0.001[c]
G2	132 (53.9)	79 (32.4)	
G3	90 (36.7)	105 (43.0)	
G4	15 (6.1)	58 (23.8)	
T stage			
T1	157 (64.1)	87 (35.7)	<0.001[b]
T2	27 (11.0)	35 (14.3)	
T3	60 (24.5)	112 (45.9)	
T4	1 (0.4)	10 (4.1)	
N stage			
N0	120 (49.0)	112 (45.9)	0.024[a]
N1	2 (0.8)	12 (4.9)	
Nx	123 (50.2)	120 (49.2)	
M stage			
M0	227 (92.7)	185 (75.8)	<0.001[b]
M1	18 (7.3)	59 (24.2)	
Outcome			
Alive	199 (81.2)	129 (52.9)	<0.001[b]
Dead	46 (18.8)	155 (47.1)	

[a]$P<0.05$, [b]$P<0.01$, [c]$P<0.001$, χ^2 test.

stage (P=0.012) and poorer OS compared with patients in the low-risk group (Table III). The levels of risk score according to different clinicopathological features were compared; significantly different risk scores were determined between patients stratified by pathological stage, histological grade, T stage, N stage and M stage in TCGA cohort (all P<0.001; Fig. 5C-H).

ROCs were used to determine the prognostic accuracy of the risk score, histological grade and pathological stage in patients with ccRCC. The results revealed that in TCGA cohort, the accuracy of the risk score [area under the curve (AUC), 0.736] was superior compared with those of histological grade (AUC, 0.681) and pathological stage (AUC, 0.720) in predicting 5-year survival (Fig. 5I). In predicting 5-year recurrence, the risk score (AUC, 0.728) was superior compared with histological grade (AUC, 0.722) but inferior to pathological

stage (AUC, 0.820) (Fig. 5J). The combination of these three characteristics improved the accuracy of predicting the 5-year survival and recurrence of the same cohort (AUC, 0.782 and 0.859, respectively). Therefore, the risk score was able to correctly predict the prognosis for patients with ccRCC.

Construction of nomograms based on the m6A-related signature. In TCGA cohort, univariate Cox regression analyses demonstrated that the risk score, pathological stage, histological grade, T, M and N stage had prognostic value in OS and DFS, whereas age was associated exclusively with OS (Fig. 6A and B). These factors were used for multivariate Cox regression analysis. The risk score, histological grade and pathological stage remained significantly associated with OS and DFS. Additionally, age, M and N stage were independent prognostic factors of OS, whereas T stage was an independent prognostic factor of DFS (Fig. 6A and B). Similar results were observed in the validation cohort, where the risk score (P=0.014) and pathological stage (P<0.001) were associated with OS in multivariate analyses (Fig. 6C).

Nomograms for 3- and 5-year OS and DFS were constructed based on the m6A-related signature and other independent prognostic factors in multivariate Cox regression analyses (Fig. 7A and B). The c-indices of nomograms were 0.783±0.018 (mean ± SEM) and 0.819±0.018 for OS and DFS, respectively, indicating that the prognostic prediction of nomograms was largely consistent with the actual OS and DFS in patients with ccRCC. Additionally, calibration plots demonstrated that nomogram prediction exhibited an agreement with actual 3-year OS and DFS (Fig. 7C and E) and a relative agreement with actual 5-year OS and DFS (Fig. 7D and F).

Validation of m6A RNA methylation by in vitro experiments. RT-qPCR was used to validate the expression levels of the seven selected m6A RNA methylation regulators in four human RCC cell lines (SW839, SN12C, 786-O and OSRC-2) and one human normal renal tubular epithelial cell line (HK-2). The results demonstrated significant differences in the expression levels of five m6A RNA methylation regulators (KIAA1429, ALKBH3, HNRNPA2B1, IGF2BP2 and METTL3) between RCC and normal renal cells (Fig. 8A). In addition, m6A RNA modification levels in the cell lines were detected. The m6A RNA modification levels in RCC cell lines SW839 and 786-O were significantly higher compared with that in HK-2 cells (Fig. 8B).

Discussion

As the most common type of adult kidney cancer, ccRCC is characterized by poor prognosis and a high risk of metastasis and recurrence (29). Epigenetic modifications, including RNA modification (21,22,24), DNA methylation (30), histone modification (31) and microRNA changes (32,33), serve diverse functions in the malignant progression and prognosis of ccRCC. As the most prevalent type of internal RNA modification, m6A RNA methylation has gained increasing attention over the past decade (5,7,8,12). At present, the functions of m6A RNA methylation regulators in ccRCC are unclear. The present study investigated the associations between the expression of these genes and clinicopathological features including prognosis, explored the potential biological processes and
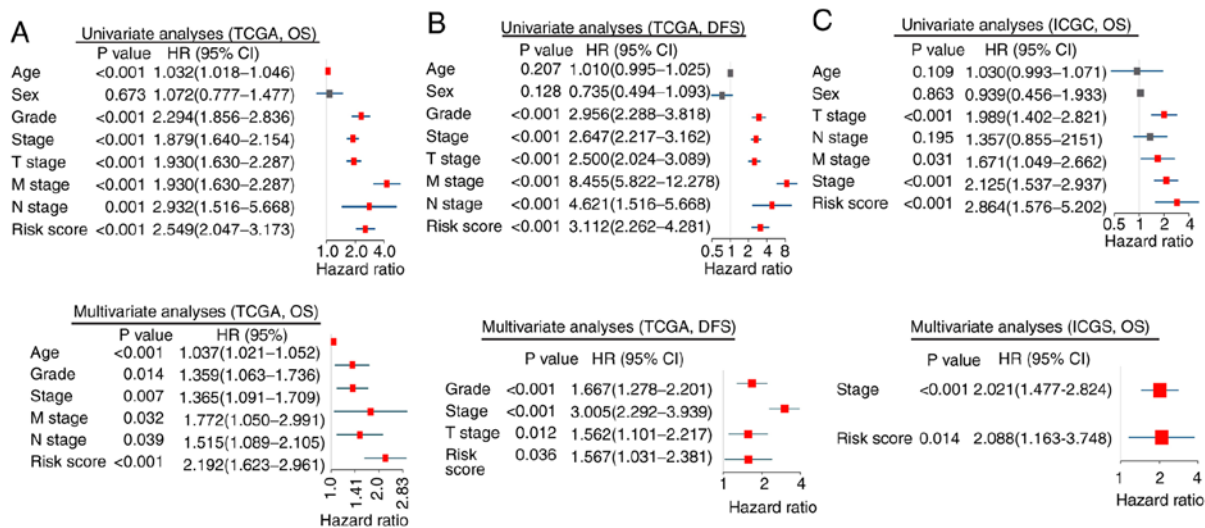
Figure 6. Univariate and multivariate Cox regression analyses. Associations between clinicopathological factors (including the risk score) and survival of patients with clear cell renal cell carcinoma in (A and B) TCGA and (C) ICGC cohorts. TCGA, The Cancer Genome Atlas; ICGC, International Cancer Genome Consortium; OS, overall survival; DFS, disease-free survival; HR, hazard ratio; CI, confidence interval.
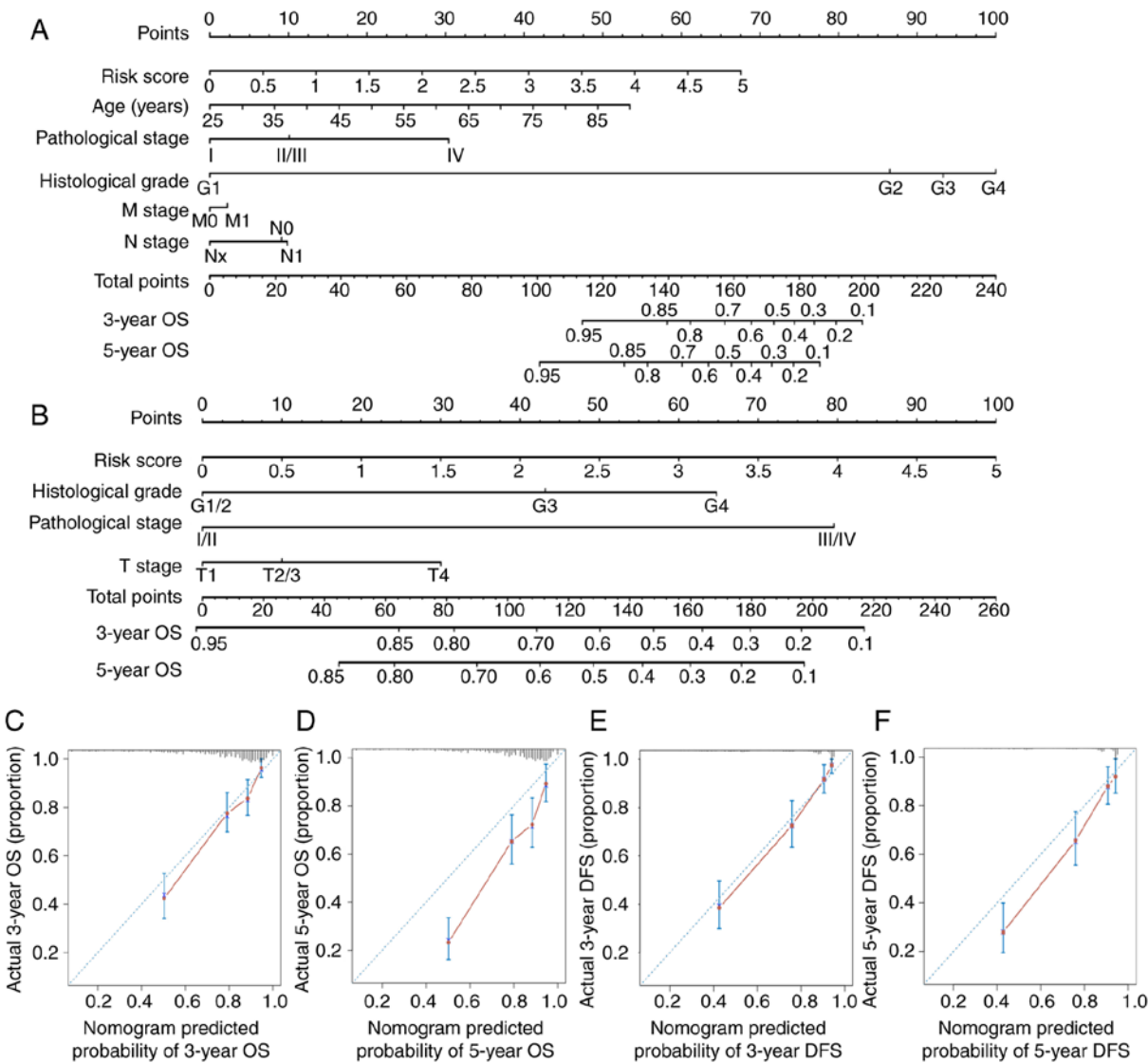

Figure 7. Nomograms for predicting the survival of patients with clear cell renal cell carcinoma in The Cancer Genome Atlas cohort. (A) Nomogram to predict 3-year and 5-year OS. (B) Nomogram to predict 3-year and 5-year DFS. Calibration plots of (C) 3-year and (D) 5-year OS nomograms. Calibration plots of (E) 3-year and (F) 5-year DFS nomograms. OS, overall survival; DFS, disease-free survival.
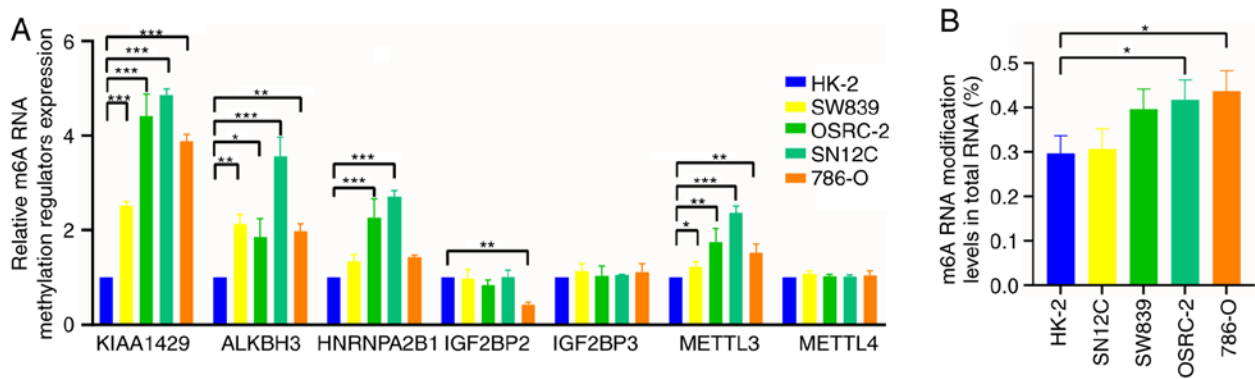
Figure 8. Validation of m6A RNA methylation through *in vitro* experiments. (A) RT-qPCR validation of seven m6A RNA methylation regulators in RCC cell lines SW839, SN12C, 786-O and OSRC-2 and normal renal tubular epithelial cell line HK-2. (B) m6A RNA modification levels in RCC cell lines and normal renal tubular epithelial cell line. *P<0.05, **P<0.01, ***P<0.001. m6A, N[6]-methyladenosine; RCC, renal cell carcinoma.

constructed a m6A-related signature and nomograms for prognostic prediction of ccRCC.

A total of 15 of the 19 analyzed m6A RNA methylation regulators were differentially expressed between ccRCC and adjacent non-tumor tissues, indicating that the m6A RNA methylation regulators served important roles in the tumorigenesis of ccRCC. Among the m6A RNA methylation regulators, 'writers' are considered to be the main regulators of m6A in ccRCC (22), and Lobo *et al* (21) reported that the mRNA deregulation of the 'writers' was associated with clinicopathological features and survival of patients with RCC. The present study also confirmed the major role of 'writers' by analyzing the network and associations among 19 m6A RNA methylation regulators. In the present study, WTAP served an important role among the 'writers' and was significantly upregulated in ccRCC tissues. In a study by Tang *et al* (24), the expression of WTAP was also significantly upregulated in RCC cell lines and tissues, and high expression of WTAP was associated with poor OS in patients with ccRCC. These results further suggested that WTAP was a hub gene among the 'writers' and served an oncogenic role in ccRCC.

A previous study has reported that WTAP can interact and colocalize with the METTL3-METTL14 heterodimer to affect m6A RNA methylation on nuclear RNA (34). The results of the present study demonstrated a wide range of interactions, especially known interactions within the 'writers', and the expression of WTAP was also associated with the expression levels of the 'writers' METTL3 and METTL14.

As members of the 'writers', METTL3 and METTL14 exhibit completely opposite functions in different types of tumors. In acute myeloid leukemia, METTL3 and METTL14 serve oncogenic roles; compared with normal hematopoietic cells, the expression of METTL3 and METTL14 is significantly upregulated in acute myeloid leukemia cells (35). By contrast, METTL3 and METTL14 are regarded as suppressor genes in glioblastoma, and knockdown of METTL3 and METTL14 promotes the growth, self-renewal and tumorigenesis of human glioblastoma stem cells (16). The oncogenic role of METTL3 has been validated in hepatocellular carcinoma (19), and the present study also revealed that METTL3 was more abundant in ccRCC compared with adjacent non-tumor tissues, and that patients with ccRCC with upregulated METTL3 exhibited a shorter OS. METTL14 acts as a suppressor gene in 7 of the 37 types of

cancer in TCGA (10). In hepatocellular carcinoma, downregulation of METTL14 can significantly promote tumor metastasis *in vivo* and *in vitro* (36). In ccRCC, the expression of METTL14 has been reported to be significantly decreased in ccRCC tissues compared with non-tumor tissues, and METTL14 may inhibit renal cancer cell migration and invasion by abrogating the expression of purinergic receptor P2RX6 (23). The results of the present study revealed that the expression of METTL14 was significantly decreased in ccRCC compared with adjacent non-tumor tissues, especially in high histological grade and high pathological stage ccRCC tissues, and patients with ccRCC with low expression of METTL14 exhibited longer OS and DFS. These results suggested that the m6A RNA methylation regulators may serve diverse roles in different tumors, and that even the same regulator may exert different effects depending on the tissue specificity. In the present study, METTL3 and METTL14 exhibited opposite functions in ccRCC, which was also reflected in the opposite values of coefficients. Although KIAA1429 was upregulated in ccRCC compared to adjacent non-tumor tissues, it was significantly prone to be upregulated in low pathological stage and low histological grade ccRCC tissues, which contributed to the negative coefficient and its role as a suppressor gene in ccRCC.

The 'reader' genes IGF2BP1, IGF2BP2, IGFBP3 and HNRNPA2B1 were upregulated in high pathological stage and high histological grade ccRCC tissues. In addition, upregulation of each gene was significantly associate with poor OS or DFS. The oncogenic features of these four genes also have been identified in at least seven types of cancer based on the 33 types of cancer in TCGA (10). Among them, IGF2BP3 functions as an oncogene in 13 of the 33 types of cancer in TCGA and 33 cohorts across seven types of tissues in the Gene Expression Omnibus. HNRNPA2B1 is associated with a high risk in nine types of cancer and a proactive role in four types of cancer in TCGA (10). However, only IGF2BP2, IGF2BP3 and HNRNPA2B1 were selected by LASSO Cox regression analyses to build the m6A-related signature. Of note, IGF2BP1, IGF2BP2 and IGF2BP3 were positively associated with each other (Fig. 5A), which may attribute to the removal of IGF2BP1 as a factor.

The expression levels of the m6A methylation 'erasers' FTO, ALKBH3 and ALKBH5 in ccRCC tissues were higher compared with those in adjacent non-tumor tissues, although their expression levels were not associated with the histological grade

and pathological stage of ccRCC, and only patients with high expression levels of ALKBH3 exhibited a poor prognosis. Thus, ALKBH3 was the only 'eraser' selected for further analysis.

According to the expression similarities of the m6A RNA methylation regulators in the present study, the patients from TCGA cohort were divided into three clusters by consensus clustering. GO and KEGG analyses demonstrated that the clustering results were closely associated with the malignancy of ccRCC via RNA metabolism and malignancy-related pathways, including primary immunodeficiency, regulation of autophagy and response to oxidative stress. The m6A RNA methylation regulators can influence almost every step of RNA metabolism (11), and their alteration is associated with the alterations of p53 and VHL (7,22). Due to the vital roles of RNA biology, p53 and VHL in the development of ccRCC (32,37), the dysregulated expression of the m6A RNA methylation regulators may result in abnormal RNA metabolism and alteration of p53 and VHL, which may affect the initiation and progression of ccRCC. The results of the bioinformatics analysis in the present study were in accordance with this assumption.

Building a risk signature based on the expression levels of m6A RNA methylation regulators may help predict the clinical survival outcomes of patients with ccRCC, which is regarded as a vital topic of research (9,10,17). The present study constructed a m6A-related risk signature, which achieved good performance in prognostic stratification in the training (TCGA) and validation (ICGC) cohorts. In addition, the risk signature correctly predicted the prognosis and stratified the OS and DFS for patients with ccRCC with different histological grades and pathological stages. This m6A-related risk signature and other independent prognostic factors were used to build nomograms for 3- and 5-year OS and DFS. Calibration plots and the c-indices revealed that the prognostic prediction of the nomograms was largely consistent with the actual OS and DFS, especially the actual 3-year OS and DFS. Nomograms based on the m6A-related risk signature may serve as a useful evaluation tool to perform personalized recurrence and mortality risk identification in patients with ccRCC.

The results of RT-qPCR in the present study indicated that five of the seven m6A RNA methylation regulators exhibited dysregulated expression between RCC cell lines and a normal renal tubular epithelial cell line, suggesting that dysregulated expression levels of m6A RNA methylation regulators served an important role in the carcinogenesis of ccRCC. The 'writer' genes KIAA1429 and METTL3 were upregulated in RCC cell lines compared with the normal renal tubular epithelial cell line. It has been reported that the upregulation of 'writers', including KIAA1429 and METTL3, is associated with invasiveness of cancer cells, aggressive clinicopathological features and poor prognosis in lung, liver, gastric and prostate cancer (7,19,21,38-40). Mechanistically, this could partially explain the result of the present study that m6A RNA modification levels were higher in RCC cell lines compared with the normal renal tubular epithelial cell line. A similar increase in the levels of m6A RNA modification was also reported in gastric, prostate and pancreatic cancer (39-41). Thus, higher levels of m6A RNA modification in total RNA may result in the development of cancer-related features.

In conclusion, the present study systematically demonstrated the prevalent dysregulated expression, biological function and prognostic value of m6A RNA methylation regulators in ccRCC. The dysregulated expression of the m6A RNA methylation regulators was associated with differential expression of genes enriched in RNA metabolism- and malignancy-related pathways. In future studies, methylated m6A RNA immunoprecipitation sequencing and m6A-sequencing may help identify the definite target mRNAs of the m6A RNA modifications during ccRCC initiation and progression. For clinical practices, the present study constructed m6A-related nomograms that effectively predicted the outcome of patients with ccRCC. Dysregulated expression of the m6A RNA methylation regulators and dysregulated m6A RNA methylation levels were also validated in multiple RCC cells by *in vitro* experiments. Functional studies and mechanistic analyses of m6A regulators may be helpful to the development of m6A-targeted treatments for ccRCC.

Availability of data and materials

Data of the mRNA expression of m6A RNA methylation regulators and corresponding clinicopathological features were retrieved from TCGA (http://cancergenome.nih.gov/) and ICGC (https://icgc.org/), which are openly available.

Authors' contributions

ZTZ and XDY conceived and designed the study. XDY acquired the funding. ZTZ, SYM and YDG collected and collated the data. All authors were involved in the analysis and interpretation of data. ZTZ and SYM performed all the experiments. ZTZ wrote the manuscript. XDY, SYM and WTZ critically reviewed and revised the manuscript. JL and CL designed the tables and figures. All authors read and approved the manuscript and agree to be accountable for all aspects of the research in ensuring that the accuracy or integrity of any part of the work were appropriately investigated and resolved.

Ethics approval and consent to participate

Not applicable.

Patient consent for publication

Not applicable.

Competing interests

The authors declare that they have no competing interests.

References

1. Boccaletto P, Machnicka MA, Purta E, Piatkowski P, Baginski B, Wirecki TK, de Crecy-Lagard V, Ross R, Limbach PA, Kotter A, et al: MODOMICS: A database of RNA modification pathways. 2017 update. Nucleic Acids Res 46: D303-D307, 2018.

2. Lewis CJ, Pan T and Kalsotra A: RNA modifications and structures cooperate to guide RNA-protein interactions. Nat Rev Mol Cell Biol 18: 202-210, 2017.

3. Gilbert WV, Bell TA and Schaening C: Messenger RNA modifications: Form, distribution, and function. Science 352: 1408-1412, 2016.

4. Karijolich J, Kantartzis A and Yu YT: RNA Modifications: A Mechanism that Modulates Gene Expression. Methods Mol Biol 629: 1-19, 2010.

5. Wang S, Sun C, Li J, Zhang E, Ma Z, Xu W, Li H, Qiu M, Xu Y, Xia W, et al: Roles of RNA methylation by means of N6-methyladenosine (m6A) in human cancers. Cancer Lett 408: 112-120, 2017.

6. Desrosiers R, Friderici K and Rottman F: Identification of methylated nucleosides in messenger RNA from Novikoff hepatoma cells. Proc Natl Acad Sci USA 71: 3971-3975, 1974.

7. Dominissini D, Moshitch-Moshkovitz S, Schwartz S, Salmon-Divon M, Ungar L, Osenberg S, Cesarkas K, Jacob-Hirsch J, Amariglio N, Kupiec M, et al: Topology of the human and mouse m6A RNA methylomes revealed by m6A-seq. Nature 485: 201-206, 2012.

8. Meyer KD, Saletore Y, Zumbo P, Elemento O, Mason CE and Jaffrey SR: Comprehensive analysis of mRNA methylation reveals enrichment in 3' UTRs and near stop codons. Cell 149: 1635-1646, 2012.

9. Sun T, Wu R and Ming L: The role of m6A RNA methylation in cancer. Biomed Pharmacother 112: 108613, 2019.

10. Li Y, Xiao J, Bai J, Tian Y, Qu Y, Chen X, Wang Q, Li X, Zhang Y and Xu J: Molecular characterization and clinical relevance of m6A regulators across 33 cancer types. Mol Cancer 18: 137, 2019.

11. Dai D, Wang H, Zhu L, Jin H and Wang X: N6-methyladenosine links RNA metabolism to cancer progression. Cell Death Dis 9: 124, 2018.

12. Niu Y, Zhao X, Wu YS, Li MM, Wang XJ and Yang YG: N6-methyl-adenosine (m6A) in RNA: An old modification with a novel epigenetic function. Genomics Proteomics Bioinformatics 11: 8-17, 2013.

13. Fustin JM, Doi M, Yamaguchi Y, Hida H, Nishimura S, Yoshida M, Isagawa T, Morioka MS, Kakeya H, Manabe I, et al: RNA-methylation-dependent RNA processing controls the speed of the circadian clock. Cell 155: 793-806, 2013.

14. Geula S, Moshitch-Moshkovitz S, Dominissini D, Mansour AA, Kol N, Salmon-Divon M, Hershkovitz V, Peer E, Mor N, Manor YS, et al: Stem cells. m6A mRNA methylation facilitates resolution of naive pluripotency toward differentiation. Science 347: 1002-1006, 2015.

15. Xiang Y, Laurent B, Hsu CH, Nachtergaele S, Lu Z, Sheng W, Xu C, Chen H, Ouyang J, Wang S, et al: RNA m6A methylation regulates the ultraviolet-induced DNA damage response. Nature 543: 573-576, 2017.

16. Cui Q, Shi H, Ye P, Li L, Qu Q, Sun G, Sun G, Lu Z, Huang Y, Yang CG, et al: m6A RNA methylation regulates the self-renewal and tumorigenesis of glioblastoma stem cells. Cell Rep 18: 2622-2634, 2017.

17. Chai RC, Wu F, Wang QX, Zhang S, Zhang KN, Liu YQ, Zhao Z, Jiang T, Wang YZ and Kang CS: m6A RNA methylation regulators contribute to malignant progression and have clinical prognostic impact in gliomas. Aging 11: 1204-1225, 2019.

18. Li Z, Weng H, Su R, Weng X, Zuo Z, Li C, Huang H, Nachtergaele S, Dong L, Hu C, et al: FTO plays an oncogenic role in acute myeloid leukemia as a N6-methyladenosine RNA demethylase. Cancer Cell 31: 127-141, 2017.

19. Chen M, Wei L, Law CT, Tsang FH, Shen J, Cheng CL, Tsang LH, Ho DW, Chiu DK, Lee JM, et al: RNA N6-methyladenosine methyltransferase-like 3 promotes liver cancer progression through YTHDF2-dependent posttranscriptional silencing of SOCS2. Hepatology 67: 2254-2270, 2018.

20. Zhang C, Samanta D, Lu H, Bullen JW, Zhang H, Chen I, He X and Semenza GL: Hypoxia induces the breast cancer stem cell phenotype by HIF-dependent and ALKBH5-mediated m6A-demethylation of NANOG mRNA. Proc Natl Acad Sci USA 113: E2047-E2056, 2016.

21. Lobo J, Barros-Silva D, Henrique R and Jeronimo C: The emerging role of epitranscriptomics in cancer: Focus on urological tumors. Genes (Basel) 9: pii: E552, 2018.

22. Zhou J, Wang J, Hong B, Ma K, Xie H, Li L, Zhang K, Zhou B, Cai L and Gong K: Gene signatures and prognostic values of m6A regulators in clear cell renal cell carcinoma-a retrospective study using TCGA database. Aging (Albany NY) 11: 1633-1647, 2019.

23. Gong D, Zhang J, Chen Y, Xu Y, Ma J, Hu G, Huang Y, Zheng J, Zhai W and Xue W: The m6A-suppressed P2RX6 activation promotes renal cancer cells migration and invasion through ATP-induced Ca2+ influx modulating ERK1/2 phosphorylation and MMP9 signaling pathway. J Exp Clin Cancer Res 38: 233, 2019.

24. Tang J, Wang F, Cheng G, Si S, Sun X, Han J, Yu H, Zhang W, Lv Q, Wei JF and Yang H: Wilms' tumor 1-associating protein promotes renal cell carcinoma proliferation by regulating CDK2 mRNA stability. J Exp Clin Cancer Res 37: 40, 2018.

25. Ghosh A and Barman S: Application of Euclidean distance measurement and principal component analysis for gene identification. Gene 583: 112-120, 2016.

26. Senbabaoglu Y, Michailidis G and Li JZ: Critical limitations of consensus clustering in class discovery. Sci Rep 4: 6207, 2014.

27. Simon N, Friedman J, Hastie T and Tibshirani R: Regularization paths for cox's proportional hazards model via coordinate descent. J Stat Softw 39: 1-13, 2011.

28. Livak KJ and Schmittgen TD: Analysis of relative gene expression data using real-time quantitative PCR and the 2(-Delta Delta C(T)) Method. Methods 25: 402-408, 2001.

29. Amin MB, Amin MB, Tamboli P, Javidan J, Stricker H, de-Peralta Venturina M, Deshpande A and Menon M: Prognostic impact of histologic subtyping of adult renal epithelial neoplasms: An experience of 405 cases. Am J Surg Pathol 26: 281-291, 2002.

30. Ricketts CJ, Morris MR, Gentle D, Brown M, Wake N, Woodward ER, Clarke N, Latif F and Maher ER: Genome-wide CpG island methylation analysis implicates novel genes in the pathogenesis of renal cell carcinoma. Epigenetics 7: 278-290, 2012.

31. Mosashvilli D, Kahl P, Mertens C, Holzapfel S, Rogenhofer S, Hauser S, Buttner R, Von Ruecker A, Muller SC and Ellinger J: Global histone acetylation levels: Prognostic relevance in patients with renal cell carcinoma. Cancer Sci 101: 2664-2669, 2010.

32. Xing T and He H: Epigenomics of clear cell renal cell carcinoma: Mechanisms and potential use in molecular pathology. Chin J Cancer Res 28: 80-91, 2016.

33. Yoshino H, Yonezawa T, Yonemori M, Miyamoto K, Sakaguchi T, Sugita S, Osako Y, Tatarano S, Nakagawa M and Enokida H: Downregulation of microRNA-1274a induces cell apoptosis through regulation of BMPR1B in clear cell renal cell carcinoma. Oncol Rep 39: 173-181, 2018.

34. Liu J, Yue Y, Han D, Wang X, Fu Y, Zhang L, Jia G, Yu M, Lu Z, Deng X, et al: A METTL3-METTL14 complex mediates mammalian nuclear RNA N6-adenosine methylation. Nat Chem Biol 10: 93-95, 2014.

35. Weng H, Huang H, Wu H, Qin X, Zhao BS, Dong L, Shi H, Skibbe J, Shen C, Hu C, et al: METTL14 inhibits hematopoietic stem/progenitor differentiation and promotes leukemogenesis via mRNA m6A Modification. Cell Stem Cell 22: 191-205.e9, 2018.

36. Ma JZ, Yang F, Zhou CC, Liu F, Yuan JH, Wang F, Wang TT, Xu QG, Zhou WP and Sun SH: METTL14 suppresses the metastatic potential of hepatocellular carcinoma by modulating N6-methyladenosine-dependent primary MicroRNA processing. Hepatology 65: 529-543, 2017.

37. Harlander S, Schonenberger D, Toussaint NC, Prummer M, Catalano A, Brandt L, Moch H, Wild PJ and Frew IJ: Combined mutation in Vhl, Trp53 and Rb1 causes clear cell renal cell carcinoma in mice. Nat Med 23: 869-877, 2017.

38. Lan T, Li H, Zhang D, Xu L, Liu H, Hao X, Yan X, Liao H, Chen X, Xie K, et al: KIAA1429 contributes to liver cancer progression through N6-methyladenosine-dependent post-transcriptional modification of GATA3. Mol Cancer 18: 186, 2019.

39. Cai J, Yang F, Zhan H, Situ J, Li W, Mao Y and Luo Y: RNA m6A Methyltransferase METTL3 promotes the growth of prostate cancer by regulating hedgehog pathway. Onco Targets Ther 12: 9143-9152, 2019.

40. Liu T, Yang S, Sui J, Xu SY, Cheng YP, Shen B, Zhang Y, Zhang XM, Yin LH, Pu YP and Liang GY: Dysregulated N6-methyladenosine methylation writer METTL3 contributes to the proliferation and migration of gastric cancer. J Cell Physiol 235: 548-562, 2019.

41. Xia T, Wu X, Cao M, Zhang P, Shi G, Zhang J, Lu Z, Wu P, Cai B, Miao Y and Jiang K: The RNA m6A methyltransferase METTL3 promotes pancreatic cancer cell proliferation and invasion. Pathol Res Pract 215: 152666, 2019.